HHS Public Access

Author manuscript

J Mol Cell Cardiol. Author manuscript; available in PMC 2017 April 01.

Published in final edited form as:

J Mol Cell Cardiol. 2016 April ; 93: 98–105. doi:10.1016/j.yjmcc.2016.02.020.

RSK3 is required for concentric myocyte hypertrophy in an activated Raf1 model for Noonan syndrome

Catherine L. Passariello, **Eliana C. Martinez**, **Hrishikesh Thakur**, **Maria Cesareo**, **Jinliang Li**, and **Michael S. Kapiloff***

Cardiac Signal Transduction and Cellular Biology Laboratory, Interdisciplinary Stem Cell Institute, Departments of Pediatrics and Medicine, Leonard M. Miller School of Medicine, University of Miami, Miami, FL 33101, United States

Abstract

Noonan syndrome (NS) is a congenital disorder resulting from mutations of the Ras-Raf signaling pathway. Hypertrophic cardiomyopathy associated with *RAF1* "RASopathy" mutations is a major risk factor for heart failure and death in NS and has been attributed to activation of MEK1/2-ERK1/2 mitogen-activated protein kinases. We recently discovered that type 3 p90 ribosomal S6 kinase (RSK3) is an ERK effector that is required, like ERK1/2, for concentric myocyte hypertrophy in response to pathological stress such as pressure overload. In order to test whether RSK3 also contributes to NS-associated hypertrophic cardiomyopathy, RSK3 knock-out mice were crossed with mice bearing the $Raf1^{L613V}$ human NS mutation. We confirmed that $Raf1^{L613V}$ knock-in confers a NS-like phenotype, including cardiac hypertrophy. Active RSK3 was increased in $Raf1^{L613V}$ mice. Constitutive *RSK3* gene deletion prevented the $Raf1^{L613V}$-dependent concentric growth in width of the cardiac myocyte and attenuated cardiac hypertrophy in female mice. These results are consistent with RSK3 being an important mediator of ERK1/2-dependent growth in RASopathy. In conjunction with previously published data showing that RSK3 is important for pathological remodeling of the heart, these data suggest that targeting of this downstream MAP-kinase pathway effector should be considered in the treatment of RASopathy-associated hypertrophic cardiomyopathy.

Keywords

Heart failure; Hypertrophy; Noonan Syndrome; Remodeling; Signal transduction

* Corresponding author at: Cardiac Signal Transduction and Cellular Biology Laboratory, Interdisciplinary Stem Cell Institute, University of Miami Miller School of Medicine, R198, P.O. Box 016960, Miami, FL 33101, United States. mkapiloff@med.miami.edu (M.S. Kapiloff)..

Disclosures

Drs. Kapiloff, Li, and Passariello are co-inventors of intellectual property concerning the use of RSK3 inhibitors for the treatment of heart failure, for which a patent is pending and by which they and the University of Miami may gain royalties from future commercialization. Dr. Kapiloff is the Manager of Anchored RSK3 Inhibitors, LLC, and President of Cardiac RSK3 Inhibitors, LLC, companies interested in developing RSK3 targeted therapies and in which Dr. Kapiloff holds equity.

Appendix A. Supplementary data

Supplementary data to this article can be found online at http://dx.doi.org/10.1016/j.yjmcc.2016.02.020.

1. Introduction

The RASopathies are a class of developmental disorders caused by germline mutations of the Ras/mitogen-activated protein kinase (MAPK) pathway [1]. The autosomal dominant disorder Noonan syndrome (NS) is the most common RASopathy, affecting approximately 1 in 1000–2500 newborns [2]. NS is distinguished by craniofacial features that include a prominent forehead, hypertelorism, down-slanting palpebral fissures, and low-set, posteriorly rotated ears. Other characteristics are mild or no cognitive impairment, short stature, bleeding disorders, cryptorchidism in boys, an increased risk of cancer, and, notably, heart defects, including pulmonary stenosis (50–60% of NS patients), hypertrophic cardiomyopathy (HCM, 20%), and atrial septal defects (6–10%) [1,2]. Life expectancy is lower for NS patients with HCM [3]. Congestive heart failure is more likely to be present at diagnosis (24%) than for other causes of HCM and constitutes an important risk factor for mortality in NS children [2,4]. For example, NS infants diagnosed with HCM and heart failure before 6 months of age have only a 31% 1-year survival rate [4].

NS is caused by mutations in multiple genes related to Ras signaling, including: *PTPN11* (50% of all NS), *SOS1* (~10%), *RAF1* (3–5%), *KRAS* (1–2%), *NRAS, SHOC2, CBL* and *RIT1* (<1%) [2,5–7]. The *RAF1* gene (a.k.a. CRAF) encodes a serine/threonine-specific protein kinase and Ras effector that activates the canonical MEK1/2-ERK1/2 signaling pathway. Although NS patients with *PTPN11* mutations rarely develop HCM, the incidence of HCM in patients with *RAF1* mutations is especially high (75%) [2], in particular for those *RAF1* mutations that increase ERK activity (90%) [8]. The activating $RAF1^{L613V}$ missense mutation has been identified in patients with NS and Noonan Syndrome with multiple lentigines (LEOPARD syndrome) [9,10]. The phenotype of $Raf1^{L613V/+}$ knock-in mice is similar to that for human NS, including short stature, craniofacial and hematologic abnormalities, and HCM without valvuloseptal defects [6].

Recently, we discovered that like ERK1/2, the ERK effector type 3 p90 ribosomal S6 kinase (RSK3, a.k.a. Rps6ka2) promotes the “concentric” growth in width of cardiac myocytes in vivo [11,12]. RSK3 is a member of the p90RSK serine/threonine protein kinase family [13]. All RSK isoforms (RSK1-4) contain two kinase domains, an N-terminal kinase domain (NTKD) and a C-terminal kinase domain (CTKD). Following activation by sequential RSK phosphorylation by ERK (1, 2, or 5), the CTKD (autophosphorylation), and 3-phosphoinositide-dependent protein kinase 1, it is the NTKD that phosphorylates RSK substrates. As a result, the rate-limiting step in RSK activation is ERK pathway stimulation [13]. Given the association of *RAF1* mutations that increase ERK1/2 signaling with HCM, we considered that RSK3 might be a mediator of hypertrophic signaling in NS, potentially revealing a novel therapeutic target for the treatment of syndromic HCM. We now show that active RSK3 is increased in the $Raf1^{L613V/+}$ knock-in mouse and that *RSK3* gene deletion will prevent the concentric myocyte growth associated with this NS mouse model. Although comprehensive characterization of the $Raf1^{L613V/+}$ mouse cardiac phenotype revealed features that are not typically associated with human NS and that were not affected by *RSK3* gene deletion, the data shown below suggest that RSK3 targeting may be an effective alternative strategy to prevent the HCM that causes excess mortality in NS.

2. Methods

2.1. Mouse models

All experiments involving animals were approved by the Institutional Animal Care and Use Committee at the University of Miami. The *RSK3*$^{-/-}$ C57BL/6 mouse that we previously described was mated to the *Raf1*$^{L613V/+}$ 129S6 × C57BL/6 mixed background mouse, and acquired from the Mutant Mouse Resource Research Center at the University of California, Davis (B6N;129S6-*Raf1*$^{tm1.1Bgn}$/Mmucd, stock number - 036521-UCD) [6,11]. Mice were not backcrossed into a pure C57BL/7 background as Wu et al. reported that this knock-in mutation, like *Ptpn11* mutant NS models, does not yield live mice after multiple backcrossing [6]. All mice studied were littermates from *RSK3*$^{-/+}$ × *RSK3*$^{-/+}$;*Raf1*$^{L613V/+}$ breedings, resulting in the following four cohorts: wildtype (WT), *RSK3*$^{-/-}$, *Raf1*$^{L613V/+}$, and *RSK3*$^{-/-}$;*Raf1*$^{L613V/+}$. Genotyping was performed at weaning by tail biopsy and PCR using the primers L613V-Ias (CTCCTGTTGATTTTCGGTAC) and Raf1-s (CTTCATCCTTACAGGCCCCA) that provide a PCR product only for the *Raf1*^{L613V} allele (Supplementary Fig. 1). *RSK3* genotyping was as previously described [11]. All four genotypes were present according to typical Mendelian proportions (χ^2-test, $p > 0.05$), and no excess mortality was noted during the study. Male and female mice were studied separately.

2.2. Statistics

For all experiments, *n* refers to the number of individual mice. All data are expressed as mean ± s.e.m. Comparisons among groups were assessed by one-way ANOVA followed by Tukey post-hoc testing unless otherwise indicated. The results of post-hoc testing were considered significant when $p \leq 0.05$. Repeated symbols represent *p*-values of different orders of magnitude: *$p \leq 0.05$, **$p < 0.01$, and ***$p < 0.001$. Symbols were used as follows: $^{\dagger}p$-value vs. WT; $^{\S}p$-value vs. *RSK3*$^{-/-}$; *p-value vs. *Raf1*$^{L613V/+}$; and $^{\ddagger}p$-value for ANOVA. All statistical analyses were performed using GraphPad Prism® software version 6.05 for Windows (GraphPad Software, San Diego, CA, USA). All morphometric measurements were performed by blinded investigators.

3. Results

3.1. Active RSK3 is increased in a Noonan syndrome mouse model

Activation of protein kinases can be determined using phospho-specific antibodies for residues on the activation loop of their catalytic domains [11]. To confirm the activation of ERK1/2 signaling in the *Raf1*$^{L613V/+}$ NS model, total and phospho-MEK1/2 and ERK1/2 were detected by western blot in whole heart extracts from 8 week-old mice (Fig. 1A). Both MEK1/2 and ERK1/2 total protein and activation loop phosphorylation tended to be increased in *Raf1*$^{L613V/+}$ hearts, with the 47% increase in phospho-ERK1/2 achieving statistical significance ($p = 0.05$). Interestingly, the increase in canonical ERK1/2 signaling was dependent upon RSK3 expression, such that phospho-ERK1/2 levels in *Raf1*$^{L613V/+}$ hearts was significantly reduced following RSK3 KO. RSK3 is not reliably detectable by western blotting of whole heart extracts due to the greater expression of other RSK isoforms in that tissue [11]. Instead, RSK3 was detected by western assay following

immunoprecipitation with a RSK3-specific antibody (Fig. 1B). Activated, phosphorylated RSK3 was increased 42% in *Raf1*$^{L613V/+}$ heart tissue ($p = 0.006$), consistent with up-regulation of this signaling pathway.

3.2. Raf1^{L613V} cardiac phenotype

By echocardiography, the left ventricular morphology of *Raf1*$^{L613V/+}$ mice varied with sex and age. Female *Raf1*$^{L613V/+}$ mice had a mixed dilated (eccentric) and hypertrophic (concentric) phenotype that featured a conserved diastolic left ventricular (LV) internal diameter to wall thickness ratio [ID:(PW + AW)] ratio at 4 and 16 weeks of age (Tables 1 and 2). In contrast, male *Raf1*$^{L613V/+}$ mice exhibited a dilated phenotype at 4 weeks of age without an increase in wall thickness, such that diastolic LV dimensions (LVID;d and LV Vol;d) and ID: (PW + AW) were significantly increased compared to WT mice (Supplementary Table 1), with evidence of concentric hypertrophy by 16 weeks of age (Supplementary Table 2). *RSK3*$^{-/-}$ mice were not significantly different from WT mice in ventricular dimensions, as we have previously reported [11,14]. *RSK3*$^{-/-}$;*Raf1*$^{L613V/+}$ mice exhibited an extent of LV dilation (increased LVID;d and LV Vol;d) similar to their like-gender *Raf1*$^{L613V/+}$ littermates, especially at the later time point. However, consistent with a role for RSK3 in concentric hypertrophy, RSK3 knock-out tended to oppose any *Raf1*$^{L613V/+}$-related increased in wall thickness. Female *RSK3*$^{-/-}$;*Raf1*$^{L613V/+}$ mice were smaller than their corresponding *Raf1*$^{L613V/+}$ littermates in wall thickness (LVPW;d) at 4 weeks of age and in indexed LV mass (LV Mass/BW) at both 4 and 16 weeks of age (Tables 1 and 2).

As previously published, *Raf1*^{L613V} mice tended to have an increased ejection fraction and/or fractional shortening by echocardiography (Tables 1 and 2 and Supplementary Tables 1 and 2) [6]. To define further the *Raf1*^{L613V}-associated changes in contractility, we performed left ventricular catheterization and pressure-volume loop analysis on 16-week old mice (Fig. 2, Table 3 and Supplementary Table 3). Both female and male *Raf1*^{L613V} mice exhibited dramatically increased stroke volume and cardiac output and a marked decrease in arterial elastance (afterload, Supplementary Fig. 2). The preload-independent, but afterload-dependent parameters of contractility dP/dt_{max} vs. EDV (the slope of the maximum rate of left ventricular pressure rise vs. end-diastolic volume relationship) and end-systolic elastance (Ees, slope of the end-systolic pressure-volume relationship) also tended to be decreased in the NS mouse, resulting in a normal Ea/Ees ratio. However, preload recruitable stroke work (PRSW), a contractility index that is independent of both preload and afterload [15], was unchanged in *Raf1*^{L613V} mice (Fig. 2). Diastolic function was not impaired in the *Raf1*^{L613V} mice (Table 3 and Supplementary Table 3). *RSK3* knock-out did not significantly affect hemodynamics either in the absence or the presence of the NS mutation.

In an attempt to determine the etiology of the *Raf1*^{L613V}-related low afterload, serum nitrates, complete blood counts and general chemistries were measured. No significant differences were detected between WT and *Raf1*^{L613V} mice (Supplementary Tables 4 and 5). Peripheral systolic and diastolic blood pressure were not significantly lower for both male and female *Raf1*^{L613V} mice, and pulse pressure was normal (Supplementary Table 6).

3.3. RSK3 attenuates Raf1^{L613V}-induced concentric cardiac hypertrophy

Like LV mass measured by echocardiography, indexed biventricular weight measured gravimetrically was significantly increased for 16-week old male and female *Raf1*$^{L613V/+}$ mice compared to WT controls (Table 4, Supplementary Table 7, and Fig. 3A). *RSK3* knock-out prevented the increase in overall biventricular weight only for female *Raf1*$^{L613V/+}$ mice (Fig. 3B and Table 4), consistent with the greater concentric component of the female *Raf1*$^{L613V/+}$ hypertrophy (Table 2 and Supplementary Table 2). *Raf1*^{L613V}-induced ventricular hypertrophy was associated with both significant atrial hypertrophy and increased wet lung weight, indicating mild pulmonary edema and congestive heart failure. These parameters were not significantly attenuated by *RSK3* gene deletion.

The echocardiographic and gravimetric data obtained for *RSK3*$^{-/-}$; *RAF1*$^{L613V/+}$ mice demonstrate a requirement for RSK3 in Raf1-induced concentric hypertrophy. Histologic examination using wheat germ agglutinin staining of left ventricular tissue sections revealed that *RSK3* knock-out blocked the increase in myocyte cross-section area induced by *Raf1*^{L613V} mutation for both female and male mice (Fig. 3C and Supplementary Fig. 3). Measurement of isolated female cardiac myocytes under relaxed, unloaded conditions provided further insight into the effects of these genetic alterations on myocyte morphology (Fig. 4A). *Raf1*^{L613V} myocytes were wider than control WT myocytes (16% increased mean width, Fig. 4B). While *RSK3* knock-out did not significantly affect the dimensions of WT myocytes, *RSK3* knock-out attenuated the growth in width induced by *Raf1*^{L613V} knock-in by 2/3, such that *RSK3*$^{-/-}$;*Raf1*$^{L613V/+}$ myocytes were not significantly different in width or length/width ratio from WT and *RSK3*$^{-/-}$ myocytes (Fig. 4C). There was no significant difference in myocyte length among the four cohorts. Together, these results demonstrated that RSK3 expression is required for the concentric myocyte hypertrophy induced by the *Raf1* activating mutation.

3.4. Raf1^{L613V} hearts lack characteristics of pathological remodeling

As was shown previously [6], *Raf1*^{L613V} mutation was not associated with interstitial myocardial fibrosis, either in the presence or absence of RSK3, as detected by both Masson's trichrome (Fig. 3D) and Picrosirius Red staining (data not shown). Pathological remodeling is also associated with altered gene expression. We assayed the expression of a panel of genes of which the majority we previously found were altered in pressure overload-induced hypertrophy [11]. Remarkably, no genes were significantly changed in expression in the *Raf1*$^{L613V/+}$ mouse except for *Myh7* that encodes β-myosin heavy chain (Supplementary Table 7). *Myh7* expression was not significantly inhibited by *RSK3* gene deletion.

4. Discussion

HCM associated with the NS *RAF1*^{L613V} mutation is generally considered to be a direct consequence of activation of the canonical MEK1/2-ERK1/2 signaling pathway within the cardiac myocyte [2]. Our characterization of the *Raf1*$^{L613V/+}$ mouse has revealed that while this mouse model has a phenotype that does not completely replicate human NS HCM (as discussed below), RSK3 is required for the concentric myocyte hypertrophy induced by Raf1-MEK1/2-ERK1/2 activation.

In both the current study and that originally describing this NS mouse model, *Raf1*$^{L613V/+}$ mice were shown to have a mixed dilated and concentric, hypertrophic phenotype [6]. *Raf1*$^{L613V/+}$ mice exhibited signs of high output heart failure, including an increased ejection fraction, stroke volume, and cardiac output [6]. Our hemodynamics analysis revealed that the high output state was due to decreased afterload on the heart (decreased arterial elastance, Ea). The increased output was not due to increased intrinsic myocardial contractility because: 1) preload recruitable stroke work (PRSW) was the same for *Raf1*$^{L613V/+}$ and WT mice; and 2) end-systolic elastance (Ees) and dP/dt_{max} vs. EDV, two contractile indices that are afterload-dependent [15], were reduced proportionately to arterial elastance in *Raf1*$^{L613V/+}$ mice, consistent with normal ventricular-arterial coupling [16]. One difference in hemodynamics that we observed from those reported in Wu et al. was that dP/dt_{max} was not elevated for *Raf1*$^{L613V/+}$ mice in our study, perhaps due to the slight difference in mouse background strain. Despite the *Raf1*^{L613V}-associated increase in this load-dependent parameter reported by Wu et al., we assume due to the overall similarities of our findings that the mice reported in the earlier study also had normal intrinsic cardiac contractility (PRSW). However, as Wu et al. did not report load-independent parameters, the contractile state of their *Raf1*$^{L613V/+}$ mice remains ambiguous. It is unclear why *Raf1*$^{L613V/+}$ mice had decreased afterload, and these mice were neither anemic nor had elevated serum nitric oxide levels (Supplementary Tables 4 and 5). The normal *Raf1*$^{L613V/+}$ pulse pressure would be consistent with decreased arteriolar resistance due to a direct effect of the mutation on the small vessels (Supplementary Table 6). While it is beyond the scope of this study to decipher how activated Raf1 signaling might affect the peripheral vasculature, our data revealed that the *Raf1*^{L613V}-dependent decrease in afterload was not RSK3-dependent. In addition, the decreased afterload provided an explanation for the LV dilatation in *Raf1*^{L613V} knock-in mice, as high output states are associated with volume overload [17].

In contrast to the mouse model, however, NS HCM patients do not have dilated cardiomyopathy nor presumably a high output state [4]. Instead, the overriding feature of pediatric NS HCM is concentric hypertrophy with decreased internal dimensions that can result in outflow tract obstruction and/or heart failure [4]. Despite the differences in cardiac physiology between the *Raf1*$^{L613V/+}$ mouse and human NS HCM, we, nevertheless, found the knock-in mouse to be useful for studying the mechanisms underlying NS-associated hypertrophy. Female *Raf1*$^{L613V/+}$ mice were more relevant in this regard, as they exhibited less ventricular dilatation and a structural phenotype closer to that in the human disease. It is commonly observed that male rodents preferentially exhibit ventricular dilatation in response to stress when maintained on standard soy-based chow that contains high levels of phytoestrogens [18]. Accordingly, the reversal of *Raf1*$^{L613V/+}$ hypertrophy by RSK3 knock-out was quantitatively more robust for female mice. While RSK3 knock-out prevented concentric myocyte hypertrophy for both male and female *Raf1*$^{L613V/+}$ mice, RSK3 knock-out significantly attenuated overall cardiac hypertrophy only for female *Raf1*$^{L613V/+}$ mice.

The canonical Ras-Raf-MEK1/2-ERK1/2 signaling pathway has been implicated in the regulation of concentric cardiac myocyte growth, as well as myocyte survival [19]. Left ventricular hypertrophy has been induced by cardiac myocyte-specific expression of constitutively active HRas and MEK1, as well as by cardiac-specific deletion of the Ras GTPase-activating protein neurofibromin that inhibits Ras signaling [19–21]. Conversely,

both transgenic expression of dominant negative Raf1 and conditional *ERK2* knock-out inhibited hypertrophy due to pressure overload [19,22]. At the cellular level, cardiac myocytes from mice lacking all four *ERK1/2* alleles were longer and narrower than those from control animals, resulting in an eccentric, dilated cardiomyopathy and demonstrating a role for ERK1/2 signaling in promoting the concentric growth in width of myocytes [12]. *PTPN11* (Shp2) knock-out that decreased ERK1/2 activation also resulted in an elongated myocyte morphology and dilated cardiomyopathy [23]. In contrast, myocytes from constitutively active MEK1 transgenic mice were shorter and wider [12]. These results were consistent with observations that in vitro expression of activated Raf1 or MEK1 induced the growth in width of adult rat ventricular myocytes and that in vivo the MEK inhibitor PD03250901 reversed $Raf1^{L613V/+}$-induced concentric hypertrophy [6,8,12]. We now show that activated ERK1/2 was increased in the hearts of $Raf1^{L613V/+}$ mice and that $Raf1^{L613V/+}$ cardiac myocytes were wider, with a decreased length:width ratio. Notably, the concentric hypertrophy was without the concomitant induction of other markers of pathological remodeling, including fibrosis and pressure overload-associated gene expression. Thus, notwithstanding additional, peripheral effects of the $Raf1^{L613V/+}$ allele on the mouse cardiovascular system, the concentric hypertrophy of $Raf1^{L613V/+}$ cardiac myocytes in the absence of pressure overload can be explained by the activation of MEK1/2-ERK1/2 myocyte autonomous signaling directly regulating myocyte morphology.

ERK1/2 is thought to regulate myocyte growth and survival through the activation of multiple downstream effectors, including RSK protein kinases [19]. Depending upon the cell type, RSK signaling regulates transcription and translation, as well as cellular proliferation, growth, survival and motility [13]. It is established that RSK activity is induced in cultured myocytes by diverse hypertrophic agonists [24–31], as well as in explanted hearts from patients with end-stage dilated cardiomyopathy [32]. RSK family members are ubiquitously expressed, but not functionally redundant [33–36]. For example, human *RSK2* mutations cause X-linked Coffin-Lowry Syndrome characterized mainly by mental and growth retardation and skeletal and facial anomalies [37]. Nothing is known about RSK3 and human cardiac disease. We have discovered that in rodents RSK3 is an important regulator of cardiac hypertrophy and remodeling [38]. RSK3 gene deletion attenuated the concentric myocyte hypertrophy in mice subjected to pressure overload and chronic isoproterenol infusion, as well as the physiological hypertrophy induced by forced swimming, while RSK3 was not required for normal cardiac function [11,14]. In addition, RSK3 knock-out attenuated the interstitial fibrosis, cardiac dysfunction and heart failure induced by transgenic expression of a mutant sarcomeric protein (α-tropomyosin Glu180Gly) associated with Familial Hypertrophic Cardiomyopathy [14]. We now extend these findings by showing that active, phospho-RSK3 is increased in the $Raf1^{L613V/+}$ mouse. RSK3 knock-out inhibited concentric myocyte growth in this NS model as shown by the morphometry of stained tissue sections and isolated adult myocytes. Consistent with the inhibition of myocyte growth in width, RSK3 knock-out also attenuated both the increase in LV wall thickness and mass induced by the $Raf1^{L613V/+}$ allele in female mice. It is not yet known how RSK3 regulates hypertrophy, but RSK3 does contain an N-terminal nuclear localization signal and, therefore, likely controls gene expression through the phosphorylation of relevant transcription factors [13]. Potential RSK3 substrates include CCAAT/enhancer binding

protein-β (C/EBPβ), nuclear factor of activated T-cells family members (NFATc), myosin enhancer factor 2c (MEF2c) and serum response factor (SRF) that have all been implicated in the regulation of cardiac hypertrophy [13,39–42]. Interestingly, the modest, but significant increase in activated RSK3 in $Raf1^{L613V/+}$ myocardium is consistent with our previous observation that RSK3 expression is highly correlated with the hypertrophy of cultured neonatal rat ventricular myocytes [11]. Besides hypertrophy, RSK3 was required for the activation of upstream MEK1/2-ERK1/2 signaling, suggesting that $Raf1^{L613V/+}$-induced activation of both ERK1/2 and RSK3 was maintained by a positive feedback loop, as well as RSK3 potentially promoting the induction of hypertrophy by other ERK1/2 effectors.

No definitive therapies currently exist for NS. Treatment of the $Raf1^{L613V/+}$ mouse with the MEK inhibitor PD0325901 reversed much of the NS phenotype, including the altered cardiac form and function [6]. While MEK inhibitors may hold promise for NS, the unexpected obesity induced by PD0325901 therapy [6], as well as the spontaneous, fatal dilated cardiomyopathy associated with inducible ERK1/2 double knock-out [12], suggest that other therapies may ultimately be required. As a downstream MAP-kinase effector, therapeutic intervention by RSK3 inhibition is less likely to produce the severe side effects associated with the inhibition of upstream master regulators. As confirmed here, the global, constitutive RSK3 knock-out mouse has no apparent pathological phenotype [11,14]. Although the hemodynamic abnormalities present in the $Raf1^{L613V/+}$ mouse apparently result from a different (and RSK3-independent) mechanism (i.e. decreased afterload) than the human disease, the inhibition by RSK3 knock-out of $Raf1^{L613V/+}$-associated cardiac hypertrophy in female mice suggests that RSK3 targeting will be relevant to human NS. Future research to clarify the role of RSK3 in NS HCM using other models that more closely resemble human NS should now be compelling, given our identification of RSK3 as a critical mediator of Ras-Raf-MEK-ERK signaling in concentric myocyte hypertrophy.

Supplementary Material

Refer to Web version on PubMed Central for supplementary material.

Acknowledgements

This work was funded in part by National Institutes of Health Grants R01HL075398 (M.S.K.) and F32HL117537 (C.L.P.) and a Batchelor Foundation Micah Batchelor Award for Excellence in Children's Health Research (M.S.K.).

References

1. Rauen KA. The RASopathies. Annu. Rev. Genomics Hum. Genet. 2013; 14:355–369. [PubMed: 23875798]
2. Roberts AE, Allanson JE, Tartaglia M, Gelb BD. Noonan syndrome. Lancet. 2013; 381:333–342. [PubMed: 23312968]
3. Shaw AC, Kalidas K, Crosby AH, Jeffery S, Patton MA. The natural history of Noonan syndrome: a long-term follow-up study. Arch. Dis. Child. 2007; 92:128–132. [PubMed: 16990350]
4. Wilkinson JD, Lowe AM, Salbert BA, Sleeper LA, Colan SD, Cox GF, et al. Outcomes in children with Noonan syndrome and hypertrophic cardiomyopathy: a study from the Pediatric Cardiomyopathy Registry. Am. Heart J. 2012; 164:442–448. [PubMed: 22980313]

5. Martinelli S, De Luca A, Stellacci E, Rossi C, Checquolo S, Lepri F, et al. Heterozygous germline mutations in the CBL tumor-suppressor gene cause a Noonan syndrome-like phenotype. Am. J. Hum. Genet. 2010; 87:250–257. [PubMed: 20619386]
6. Wu X, Simpson J, Hong JH, Kim KH, Thavarajah NK, Backx PH, et al. MEK-ERK pathway modulation ameliorates disease phenotypes in a mouse model of Noonan syndrome associated with the Raf1(L613V) mutation. J. Clin. Invest. 2011; 121:1009–1025. [PubMed: 21339642]
7. Koenighofer M, Hung CY, McCauley JL, Dallman J, Back EJ, Mihalek I, et al. Mutations in RIT1 cause Noonan syndrome — additional functional evidence and expanding the clinical phenotype. Clin. Genet. 2015
8. Dhandapany PS, Fabris F, Tonk R, Illaste A, Karakikes I, Sorourian M, et al. Cyclosporine attenuates cardiomyocyte hypertrophy induced by RAF1 mutants in Noonan and LEOPARD syndromes. J. Mol. Cell. Cardiol. 2011; 51:4–15. [PubMed: 21440552]
9. Pandit B, Sarkozy A, Pennacchio LA, Carta C, Oishi K, Martinelli S, et al. Gain-of-function RAF1 mutations cause Noonan and LEOPARD syndromes with hypertrophic cardiomyopathy. Nat. Genet. 2007; 39:1007–1012. [PubMed: 17603483]
10. Razzaque MA, Nishizawa T, Komoike Y, Yagi H, Furutani M, Amo R, et al. Germline gain-of-function mutations in RAF1 cause Noonan syndrome. Nat. Genet. 2007; 39:1013–1017. [PubMed: 17603482]
11. Li J, Kritzer MD, Michel JJ, Le A, Thakur H, Gayanilo M, et al. Anchored p90 ribosomal S6 kinase 3 is required for cardiac myocyte hypertrophy. Circ. Res. 2013; 112:128–139. [PubMed: 22997248]
12. Kehat I, Davis J, Tiburcy M, Accornero F, Saba-El-Leil MK, Maillet M, et al. Extra-cellular signal-regulated kinases 1 and 2 regulate the balance between eccentric and concentric cardiac growth. Circ. Res. 2011; 108:176–183. [PubMed: 21127295]
13. Romeo Y, Zhang X, Roux PP. Regulation and function of the RSK family of protein kinases. Biochem. J. 2012; 441:553–569. [PubMed: 22187936]
14. Passariello CL, Gayanilo M, Kritzer MD, Thakur H, Cozacov Z, Rusconi F, et al. p90 ribosomal S6 kinase 3 contributes to cardiac insufficiency in alpha-tropomyosin Glu180Gly transgenic mice. Am. J. Physiol. Heart Circ. Physiol. 2013; 305:H1010–H1019. [PubMed: 23913705]
15. Van den Bergh A, Flameng W, Herijgers P. Parameters of ventricular contractility in mice: influence of load and sensitivity to changes in inotropic state. Pflugers Arch. 2008; 455:987–994. [PubMed: 17932685]
16. Kass DA. Age-related changes in venticular-arterial coupling: pathophysiologic implications. Heart Fail. Rev. 2002; 7:51–62. [PubMed: 11790922]
17. Anand IS, Florea VG. High output cardiac failure. Curr. Treat. Options Cardiovasc. Med. 2001; 3:151–159. [PubMed: 11242561]
18. Luczak ED, Leinwand LA. Sex-based cardiac physiology. Annu. Rev. Physiol. 2009; 71:1–18. [PubMed: 18828746]
19. Rose BA, Force T, Wang Y. Mitogen-activated protein kinase signaling in the heart: angels versus demons in a heart-breaking tale. Physiol. Rev. 2010; 90:1507–1546. [PubMed: 20959622]
20. Xu J, Ismat FA, Wang T, Lu MM, Antonucci N, Epstein JA. Cardiomyocyte-specific loss of neurofibromin promotes cardiac hypertrophy and dysfunction. Circ. Res. 2009; 105:304–311. [PubMed: 19574548]
21. Bueno OF, De Windt LJ, Tymitz KM, Witt SA, Kimball TR, Klevitsky R, et al. The MEK1-ERK1/2 signaling pathway promotes compensated cardiac hypertrophy in transgenic mice. EMBO J. 2000; 19:6341–6350. [PubMed: 11101507]
22. Ulm S, Liu W, Zi M, Tsui H, Chowdhury SK, Endo S, et al. Targeted deletion of ERK2 in cardiomyocytes attenuates hypertrophic response but provokes pathological stress induced cardiac dysfunction. J. Mol. Cell. Cardiol. 2014; 72:104–116. [PubMed: 24631771]
23. Kontaridis MI, Yang W, Bence KK, Cullen D, Wang B, Bodyak N, et al. Deletion of Ptpn11 (Shp2) in cardiomyocytes causes dilated cardiomyopathy via effects on the extracellular signal-regulated kinase/mitogen-activated protein kinase and RhoA signaling pathways. Circulation. 2008; 117:1423–1435. [PubMed: 18316486]

24. Sadoshima J, Izumo S. Mechanical stretch rapidly activates multiple signal transduction pathways in cardiac myocytes: potential involvement of an autocrine/paracrine mechanism. EMBO J. 1993; 12:1681–1692. [PubMed: 8385610]
25. Yamazaki T, Tobe K, Hoh E, Maemura K, Kaida T, Komuro I, et al. Mechanical loading activates mitogen-activated protein kinase and S6 peptide kinase in cultured rat cardiac myocytes. J. Biol. Chem. 1993; 268:12069–12076. [PubMed: 7685031]
26. Sadoshima J, Qiu Z, Morgan JP, Izumo S. Angiotensin II and other hypertrophic stimuli mediated by G protein-coupled receptors activate tyrosine kinase, mitogen-activated protein kinase, and 90-kD S6 kinase in cardiac myocytes. The critical role of Ca(2+)-dependent signaling. Circ. Res. 1995; 76:1–15. [PubMed: 8001266]
27. Kodama H, Fukuda K, Pan J, Sano M, Takahashi T, Kato T, et al. Significance of ERK cascade compared with JAK/STAT and PI3-K pathway in gp130-mediated cardiac hypertrophy. Am. J. Physiol. Heart Circ. Physiol. 2000; 279:H1635–H1644. [PubMed: 11009450]
28. Baliga RR, Pimental DR, Zhao YY, Simmons WW, Marchionni MA, Sawyer DB, et al. NRG-1-induced cardiomyocyte hypertrophy. Role of PI-3-kinase, p70(S6K), and MEK-MAPK-RSK. Am. J. Physiol. 1999; 277:H2026–H2037. [PubMed: 10564160]
29. Snabaitis AK, Muntendorf A, Wieland T, Avkiran M. Regulation of the extracellular signal-regulated kinase pathway in adult myocardium: differential roles of G(q/11), Gi and G(12/13) proteins in signalling by alpha1-adrenergic, endothelin-1 and thrombin-sensitive protease-activated receptors. Cell. Signal. 2005; 17:655–664. [PubMed: 15683740]
30. Takeishi Y, Abe J, Lee JD, Kawakatsu H, Walsh RA, Berk BC. Differential regulation of p90 ribosomal S6 kinase and big mitogen-activated protein kinase 1 by ischemia/reperfusion and oxidative stress in perfused guinea pig hearts. Circ. Res. 1999; 85:1164–1172. [PubMed: 10590243]
31. Takimoto E, Kass DA. Role of oxidative stress in cardiac hypertrophy and remodeling. Hypertension. 2007; 49:241–248. [PubMed: 17190878]
32. Takeishi Y, Huang Q, Abe J, Che W, Lee JD, Kawakatsu H, et al. Activation of mitogen-activated protein kinases and p90 ribosomal S6 kinase in failing human hearts with dilated cardiomyopathy. Cardiovasc. Res. 2002; 53:131–137. [PubMed: 11744021]
33. Zhao Y, Bjorbaek C, Weremowicz S, Morton CC, Moller DE. RSK3 encodes a novel pp90rsk isoform with a unique N-terminal sequence: growth factor-stimulated kinase function and nuclear translocation. Mol. Cell. Biol. 1995; 15:4353–4363. [PubMed: 7623830]
34. Zeniou M, Ding T, Trivier E, Hanauer A. Expression analysis of RSK gene family members: the RSK2 gene, mutated in Coffin-Lowry syndrome, is prominently expressed in brain structures essential for cognitive function and learning. Hum. Mol. Genet. 2002; 11:2929–2940. [PubMed: 12393804]
35. Lara R, Mauri FA, Taylor H, Derua R, Shia A, Gray C, et al. An siRNA screen identifies RSK1 as a key modulator of lung cancer metastasis. Oncogene. 2011; 30:3513–3521. [PubMed: 21423205]
36. Lin JX, Spolski R, Leonard WJ. Critical role for Rsk2 in T-lymphocyte activation. Blood. 2008; 111:525–533. [PubMed: 17938253]
37. Hunter AG. Coffin-Lowry syndrome: a 20-year follow-up and review of long-term outcomes. Am. J. Med. Genet. 2002; 111:345–355. [PubMed: 12210291]
38. Martinez EC, Passariello CL, Li J, Matheson CJ, Dodge-Kafka K, Reigan P, et al. RSK3: a regulator of pathological cardiac remodeling. IUBMB Life. 2015; 67:331–337. [PubMed: 25988524]
39. Bostrom P, Mann N, Wu J, Quintero PA, Plovie ER, Panakova D, et al. C/EBPbeta controls exercise-induced cardiac growth and protects against pathological cardiac remodeling. Cell. 2010; 143:1072–1083. [PubMed: 21183071]
40. Oka T, Xu J, Molkentin JD. Re-employment of developmental transcription factors in adult heart disease. Semin. Cell Dev. Biol. 2007; 18:117–131. [PubMed: 17161634]
41. Potthoff MJ, Olson EN. MEF2: a central regulator of diverse developmental programs. Development. 2007; 134:4131–4140. [PubMed: 17959722]
42. Miano JM. Role of serum response factor in the pathogenesis of disease. Lab. Investig. 2010; 90:1274–1284. [PubMed: 20498652]

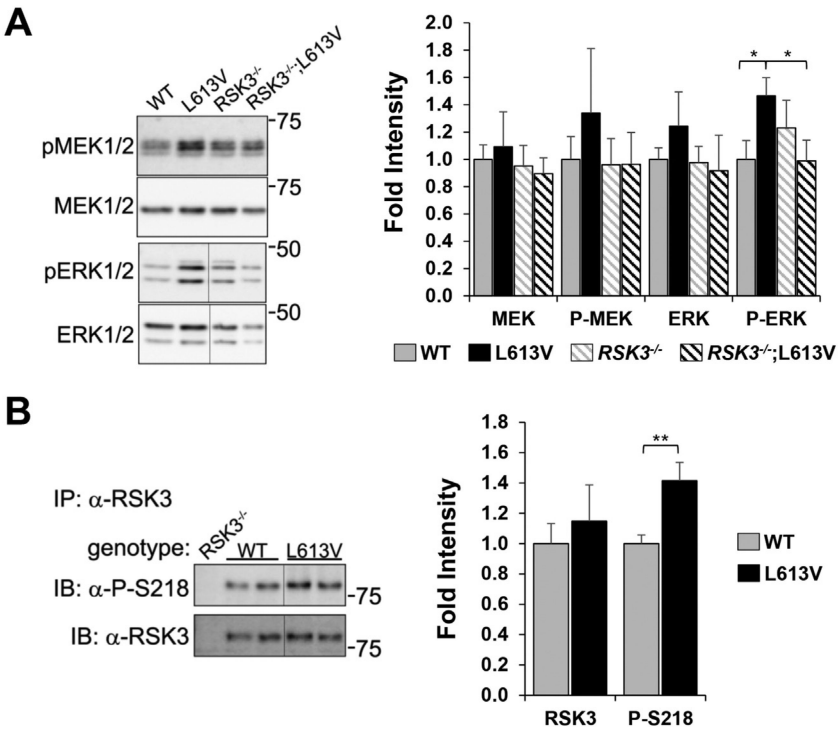

Fig. 1.

Active RSK3 was increased in the heart by expression of the activating Noonan Syndrome *Raf1*^{L613V} mutant allele. A. MEK1/2 and ERK1/2 total and phosphorylated, activated protein kinases were detected in the hearts of individual 8-week old mice with genotypes as indicated. B. RSK3 protein was immunoprecipitated from these hearts, as well as *RSK3*$^{-/-}$ negative control hearts, using N-16 RSK3-specific antibody and detected by western blotting using a phospho-Ser-218-specific antibody for activated RSK3 (top) or OR43 for total RSK3 (bottom). Vertical lines indicate where non-adjacent lanes from the same blot are shown next to each other. Densitometry of blots is shown to the right. Data shown as fold increase compared to WT mean. $n \geq 4$ mice for each panel (male and female data combined since similar). *$p \leq 0.05$; **$p \leq 0.01$ by Student's *t*-test.

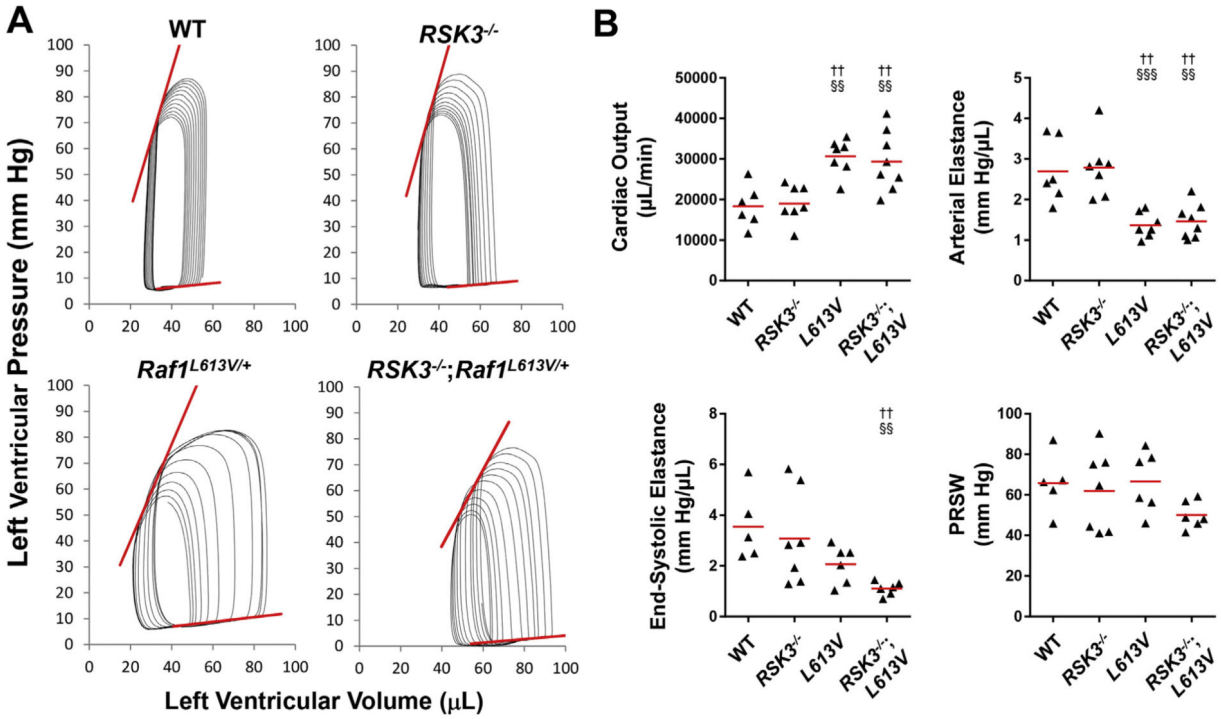

Fig. 2.

Raf1$^{L613V/+}$ mutation resulted in high cardiac output due to low afterload. A. Representative pressure-volume loops studied by left ventricular catheterization of female mice to acquire preload-independent parameters. Loop series were obtained by inferior vena cava compression following a limited right thoracotomy. See Table 3 for analysis. Red lines indicate end-systolic and end-diastolic pressure-volume relationships (ESPVR and EDPVR, respectively). B. Quantification of cardiac output, arterial elastance, end-systolic elastance (ESPVR slope) and preload recruitable stroke work (PRSW). n = 6–8 per cohort. $^{\dagger}p$-Value vs. WT; $^{\S}p$-value vs. *RSK3*$^{-/-}$.

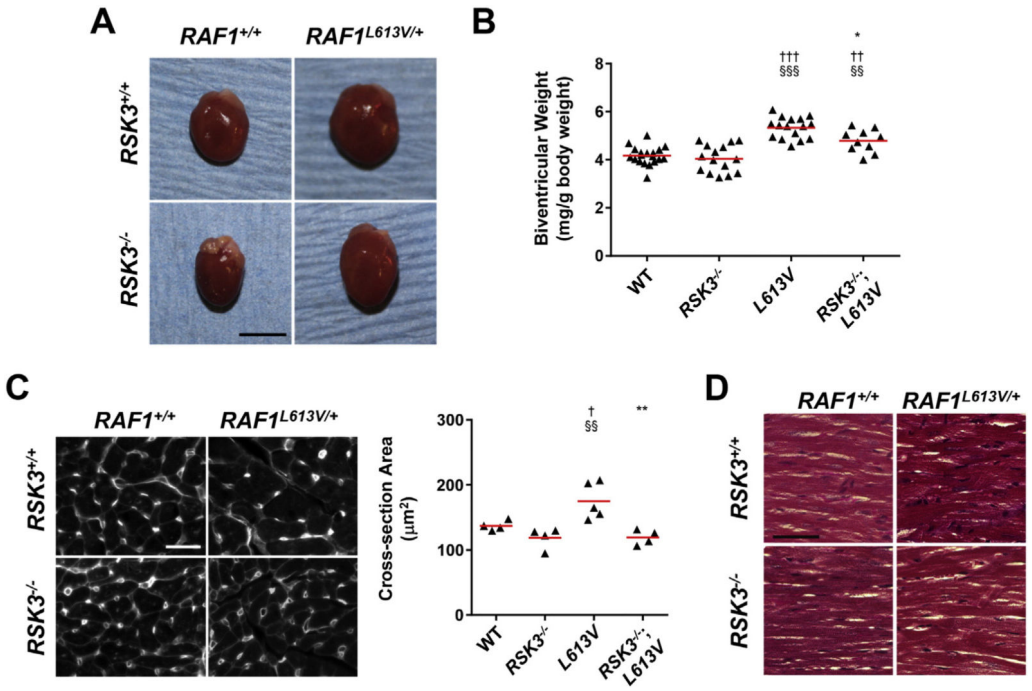

Fig. 3.

RSK3 is required for *Raf1*^{L613V}-induced cardiac hypertrophy in female mice. A. Representative female hearts at 16 weeks of age. Bar = 5 mm. B. Indexed biventricular weight. n = 10–19. C. Wheat germ agglutinin-strained heart sections (left, bar = 10 μm) and quantification of cross-section area (right). n = 4–5. D. Trichrome-staining reveals no interstitial fibrosis for any of the cohorts. Bar = 50 μm. $^{\dagger}p$-Value vs. WT; $^{\S}p$-value vs. *RSK3*$^{-/-}$; *p-value vs. *Raf1*$^{L613V/+}$.

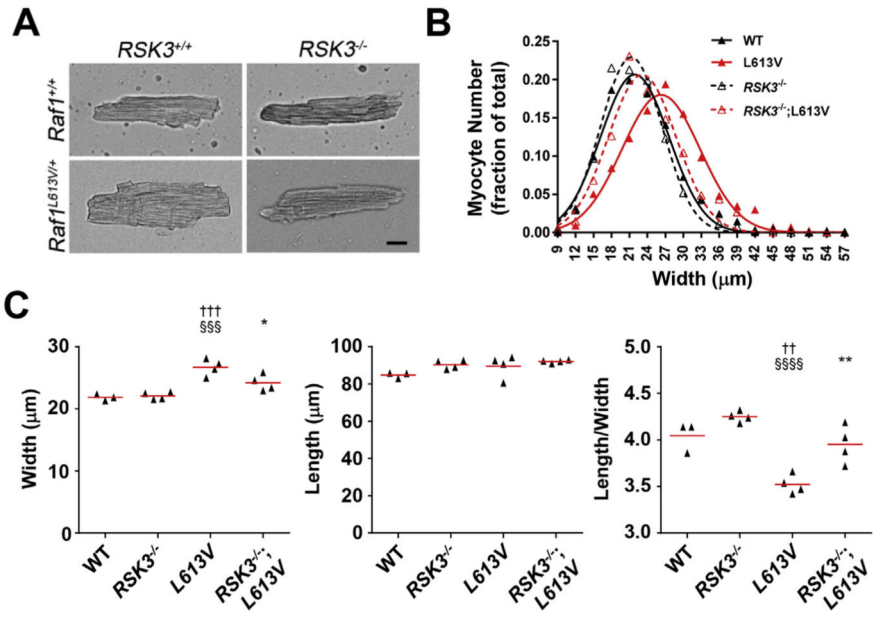

Fig. 4.

RSK3 is required for *Raf1*^{L613V}-induced myocyte hypertrophy in female mice. A. Images of dissociated female myocytes (bar = 20 μm). B. Histogram shows the aggregate distribution of myocyte widths (WT – 312 myocytes from 3 mice; *RSK3*$^{-/-}$ – 423 myocytes from 4 mice; *Raf1*$^{L613V/+}$ – 439 myocytes from 4 mice; *RSK3*$^{-/-}$; *Raf1*$^{L613V/+}$ – 412 myocytes from 4 mice). C. Mean width, length and length:width ratio for the individual mice. Red bars indicate means for cohorts. *p*-Value symbols: † vs. WT; § vs. *RSK3*$^{-/-}$; * vs. *Raf1*$^{L613V/+}$.

Table 1

Echocardiography: data – 4 week old female mice.

		WT	*RSK3*$^{-/-}$	*RAF1*$^{L613V/+}$			*RSK3*$^{-/-}$;*RAF1*$^{L613V/+}$		ANOVA
n		**22**	**15**	**16**			**8**		
LVPW;d	mm	0.57 ± 0.01	0.61 ± 0.02	0.68 ± 0.02	†††		0.58 ± 0.03	*	‡‡‡
LVPW;s	mm	0.86 ± 0.02	0.92 ± 0.03	1.03 ± 0.04	†††		0.92 ± 0.04		‡‡
LVAW;d	mm	0.65 ± 0.02	0.67 ± 0.02	0.70 ± 0.03			0.63 ± 0.04		
LVAW;s	mm	1.00 ± 0.04	1.02 ± 0.05	1.16 ± 0.05			1.00 ± 0.07		
LVID;d	mm	3.48 ± 0.05	3.59 ± 0.05	3.81 ± 0.06	†††		3.77 ± 0.11	†	‡‡‡
LVID;s	mm	2.40 ± 0.07	2.46 ± 0.09	2.49 ± 0.08			2.56 ± 0.14		
ID:(PW + AW)		2.90 ± 0.10	2.82 ± 0.10	2.80 ± 0.09			3.14 ± 0.14		
LV Vol;d	µL	51 ± 2	54 ± 2	63 ± 2	†††	§	61 ± 4	†	‡‡‡
LV Vol;s	µL	21 ± 2	22 ± 2	23 ± 2			24 ± 3		
EF	%	48 ± 4	60 ± 2	64 ± 2	††		61 ± 3		‡‡
FS	%	31 ± 1	32 ± 2	35 ± 1			32±2		
LV mass	mg	52 ± 2	59 ± 2	72 ± 3	†††	§§	60 ± 5	*a*	‡‡‡
BW	g	13.1 ± 0.4	14.0 ± 0.3	13.5 ± 0.3			13.5 ± 0.6		
LV mass/BW	mg/g	4.0 ± 0.1	4.2 ± 0.1	5.3 ± 0.2	†††	§§§	4.4 ± 0.3	*	‡‡‡

LVPW, left ventricular posterior wall thickness; LVAW, left ventricular anterior wall thickness; LVID, left ventricular internal diameter; d, diastole; s, systole; ID:(PW + AW) = LVID;d / (LVPW;d + LVAW;d); Vol, volume; EF, ejection fraction; FS, fractional shortening; BW, body weight. All data are mean ± s.e.m.

† *p*-Value vs. WT.

§ *p*-Value vs. *RSK3*$^{-/-}$.

* *p*-Value vs. *Raf1*$^{L613V/+}$.

a $p = 0.07$.

Table 2

Echocardiography data – 16 week old female mice.

		WT	*RSK3*$^{-/-}$	*RAF1*$^{L613V/+}$			*RSK3*$^{-/-}$;*RAF1*$^{L613V/+}$				ANOVA
n		**18**	**14**	**12**			**9**				
LVPW;d	mm	0.69 ± 0.03	0.71 ± 0.03	0.76 ± 0.02		§	0.73 ± 0.05				
LVPW;s	mm	1.08 ± 0.05	1.12 ± 0.05	1.25 ± 0.05			1.17 ±0.08				
LVAW;d	mm	0.90 ± 0.04	0.82 ± 0.03	0.99 ± 0.03		§§	0.90 ± 0.05				‡‡
LVAW;s	mm	1.36 ± 0.06	1.29 ± 0.06	1.65 ± 0.08	††	§§§	1.38 ± 0.07			*	‡‡‡
LVID;d	mm	3.69 ± 0.07	3.51 ± 0.11	4.18 ± 0.13	†	§§	4.16 ±0.13	†	§§		‡‡‡
LVID;s	mm	2.38 ± 0.10	2.21 ± 0.14	2.45 ± 0.16			2.67 ± 0.20				
ID:(PW + AW)		2.46 ± 0.08	2.51 ± 0.11	2.62 ± 0.19			2.64 ± 0.09				
LV Vol;d	µL	58 ± 3	52 ± 4	79 ± 5	†	§§§	78 ± 5	†	§§§		‡‡‡
LV Vol;s	µL	21 ± 2	18 ± 3	23 ± 3			28 ± 5				
EF	%	66 ± 3	67 ± 3	72 ± 3			65 ± 5				
FS	%	36 ± 2	37 ± 2	42 ± 3			36 ± 4				
LV mass	mg	82 ± 3	72 ± 3	115 ± 5	†††	§§§	104 ± 7	††	§§§		‡‡‡
BW	g	24.1 ± 1.0	24.4 ± 0.7	24.2 ± 0.6			24.8 ± 1.2				
LV Mass/BW	mg/g	3.5 ± 0.1	3.0 ± 0.1	4.7 ± 0.2	†††	§§§	4.2 ± 0.2	†	§§§	*a*	‡‡‡

LVPW, left ventricular posterior wall thickness; LVAW, left ventricular anterior wall thickness; LVID, left ventricular internal diameter; d, diastole; s, systole; ID:(PW + AW) = LVID;d / (LVPW;d + LVAW;d); Vol, volume; EF, ejection fraction; FS, fractional shortening; BW, body weight. All data are mean ± s.e.m.

$^{\dagger}p$-Value vs. WT.

$^{\S}p$-Value vs. *RSK3*$^{-/-}$.

$^{*}p$-Value vs. *Raf1*$^{L613V/+}$.

$^{a}p = 0.07$.

Table 3

Hemodynamics data – 16 week old female mice.

		WT	*RSK3*$^{-/-}$	*RAF1*$^{L613V/+}$			*RSK3*$^{-/-}$;*RAF1*$^{L613V/+}$			ANOVA
n		**6**	**7**	**7**			**8**			
HR	BPM	565 ± 15	570 ± 24	554 ± 14			545 ± 20			
ESV	µL	35 ± 1	40 ± 6	41 ± 4			49 ± 5			
EDV	µL	64 ± 5	68 ± 4	86 ± 5	†		96 ± 7	††	§§	‡‡‡
SV	µL	33 ± 4	33 ± 2	55 ± 2	††	§§	55 ± 5	††	§§	‡‡‡
CO	µL/min	18,355 ± 2094	19,039 ± 1737	30,667 ± 1645	††	§§	29,410 ± 2599	††	§§	‡‡‡
Ea	mm Hg/µL	2.7 ± 0.3	2.8 ± 0.3	1.4 ± 0.1	††	§§§	1.5 ± 0.1	††	§§	‡‡‡
Systolic function										
EF	%	51 ± 3	51 ± 5	61 ± 2			56 ± 4			
dP/dt_{max}	mm Hg/µL	9527 ± 847	8911 ± 979	7793 ± 761			6912 ± 562			
ESP	mm Hg	82 ± 3	89 ± 4	74 ± 4		§	75 ± 4		*b*	‡
Ees	mm Hg/µL	3.6 ± 0.6	3.1 ± 0.7	2.1 ± 0.3	*a*		1.1 ± 0.1	††	§§	‡
dP/dt_{max} vs. EDV	mm Hg/s/µL	137 ± 29	114 ± 23	61 ± 5	*a*		46 ± 10	†	*b*	‡‡
PRSW	mmHg	66 ± 7	62 ± 7	67 ± 6			50 ± 3			
Ea/Ees		0.8 ± 0.1	1.1 ± 0.2	0.8 ± 0.1			1.4 ± 0.2			
Diastolic function										
dP/dt_{min}	mm Hg/s	–8469 ± 277	–9679 ± 864	–6961 ± 626		§	–6687 ± 467		§§	‡‡
EDP	mm Hg	7.2 ± 0.9	7.6 ± 0.9	9.7 ± 1.6			9.1 ± 2.0			
$P@dV/dt_{max}$	mm Hg	4.9 ± 1.1	6.5 ± 0.6	6.8 ± 1.3			4.6 ± 1.6			
Tau	ms	5.6 ± 0.4	6.0 ± 0.4	6.7 ± 0.5			6.2 ± 0.6			
EDVPR	mm Hg/s/µL	0.10 ± 0.03	0.09 ± 0.02	0.06 ± 0.01			0.07 ± 0.01			

HR, heart rate; ESV, end-systolic volume; EDV, end-diastolic volume; SV, stroke volume; CO, cardiac output; Ea, arterial elastance; EF, ejection fraction; dP/dt_{max}, maximum value of the pressure derivative; ESP, end-systolic pressure; Ees, end-systolic elastance, i.e. slope of the end-systolic pressure-volume relationship (ESPVR); dP/dt_{max} vs. EDV, slope of the relationship between dP/dt_{max} and EDV; PRSW, preload-recruitable stroke work; dP/dt_{min}, minimum value of the pressure derivative; EDP, end-diastolic pressure; $P@dV/dt_{max}$, pressure at the point where the maximum volume derivative occurs (fastest filling); Tau, time constant for isovolumic relaxation (Weiss's method); EDPVR slope of end-diastolic pressure-volume relationship. Load-independent parameters (PRSW, dP/dt_{max} vs. EDV, Ees, and EDVPR) were measured following thoracotomy. All data are mean ± s.e.m.

†*p*-Value vs. WT.

§ p-Value vs. *RSK3*$^{-/-}$.

^{a} $p = 0.06$ vs. WT.

^{b} $p = 0.06$ vs. *RSK3*$^{-/-}$.

Table 4

Gravimetric data – 16 week old female mice.

		WT	*RSK3*$^{-/-}$	*RAF1*$^{L613V/+}$			*RSK3*$^{-/-}$;*RAF1*$^{L613V/+}$			ANOVA
n		**19**	**15**	**16**			**10**			
Body weight	g	23.3 ± 0.7	24.3 ± 0.8	25.3 ± 0.6			25.2 ± 0.9			
Tibial length	mm	18.3 ± 0.1	18.0 ± 0.1	17.9 ± 0.2			17.9 ± 0.1			
Biventricular weight	mg	96 ± 2	97 ± 3	135 ± 4	†††	§§§	120 ± 6	†††	§§§ *	‡‡‡
Biatrial weight	mg	5.4 ± 0.2	5.8 ± 0.4	10.2 ± 0.6	†††	§§§	9.7 ± 1.3	†††	§§§	‡‡‡
Lung weight	mg	138 ± 3	138 ± 3	167 ± 5	†††	§§	161 ± 10	†	§	‡‡‡
Biventricular weight (indexed)	mg/g BW	4.17 ± 0.09	4.04 ± 0.15	5.33 ± 0.11	†††	§§§	4.78 ± 0.15	††	§§ *	‡‡‡
Biatrial weight (indexed)	mg/g BW	0.23 ± 0.01	0.24 ± 0.02	0.40 ± 0.02	†††	§§§	0.38 ± 0.04	†††	§§§	‡‡‡
Lung weight (indexed)	mg/g BW	6.0 ± 0.2	5.7 ± 0.2	6.6 ± 0.2		§	6.4 ± 0.3			‡

BW, body weight. All data are mean ± s.e.m.

†*p*-Value vs. WT.

§*p*-Value vs *RSK3*$^{-/-}$.

**p*-Value vs. *Raf1*$^{L613V/+}$.